

# Data driven extraction of Snell traces

*Rick Ottolini*

## ABSTRACT

A Snell trace is the set of data on a gather or profile with the same time slope. A Snell trace can be modeled using an *a priori* velocity function or picked directly from the data aftering dip filter has been applied. A low artifact, velocity independent dip filter is based on Kostov and Biondi's beam stack. Snell trace extraction simultaneously picks velocity and amplitude as a function of offset angle.

## INTRODUCTION

A Snell trace is the set of data on a gather or profile with the same time slope. These data will be co-linear (Figure 1) if there is no geologic dip. A flat earth is assumed to simplify Snell trace extraction. Dipping events are then corrected by migration (Ottolini, 1983).

A Snell trace imitates a slant stack. It interpolates the data rather than integrates. Interpolation is faster and has fewer numerical problems caused by offset aliasing and truncation.

Snell traces map data from offset to time slope (i.e. ray parameter). Most types of seismic data processing can be applied to time slope converted data (Ottolini, 1986). Such processing has the advantages of separating unwanted events by time slope, distinguishing angle-dependent velocity and amplitude variations, more accurate migration of dipping events, etc.

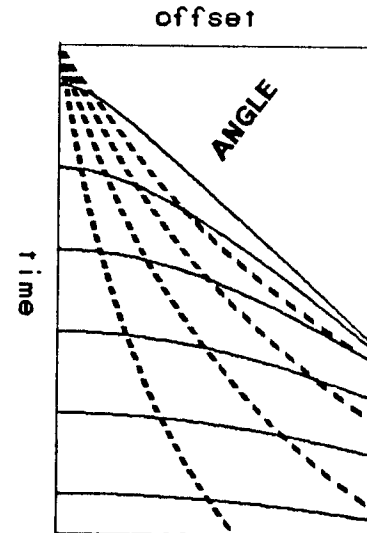


FIG. 1. Snell trace trajectories. The ray parameter increases from left to right.

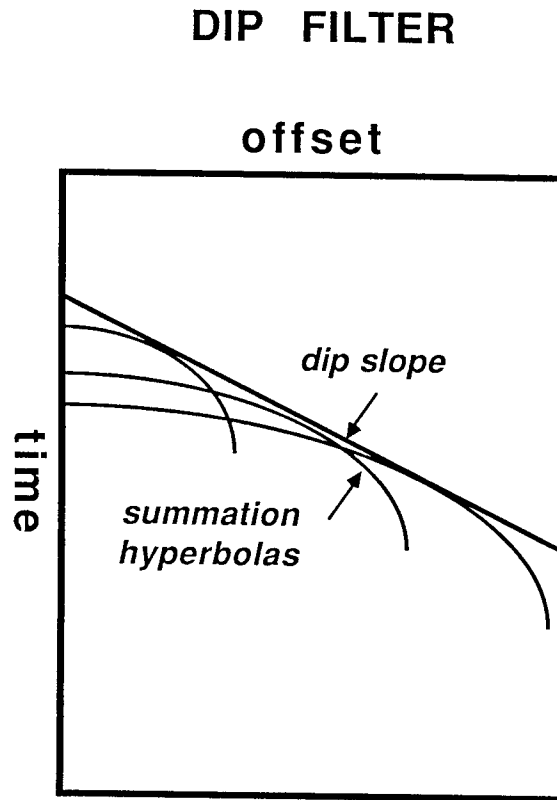


FIG. 2. Dip coherency measurement schematic. Semblance hyperbolas for a slope line at a single time point are shown. In practice, a hyperbola is computed for every point on the gather and following trace rows. The hyperbolas are computed from low to high time, then from first to last offset, following data ordering for computation efficiency.

### SNELL TRACE EXTRACTION

#### Snell trace extraction by modeling

The data moveout time  $t$  at offset  $h$  for a hyperbola with velocity  $v$  and apex time  $t_0$  is

$$t^2 = t_0^2 + \frac{h^2}{v^2}. \quad (1)$$

The time slope  $p$  is

$$\left( \frac{\partial t}{\partial h} \right)_{t,h} = p. \quad (2)$$

Ottolini (1983) solved these equations for the coordinates of a Snell trace, given a velocity  $v$

$$h = pv^2 t_0 \left( 1 - p^2 v^2 \right)^{1/2}, \quad (3)$$

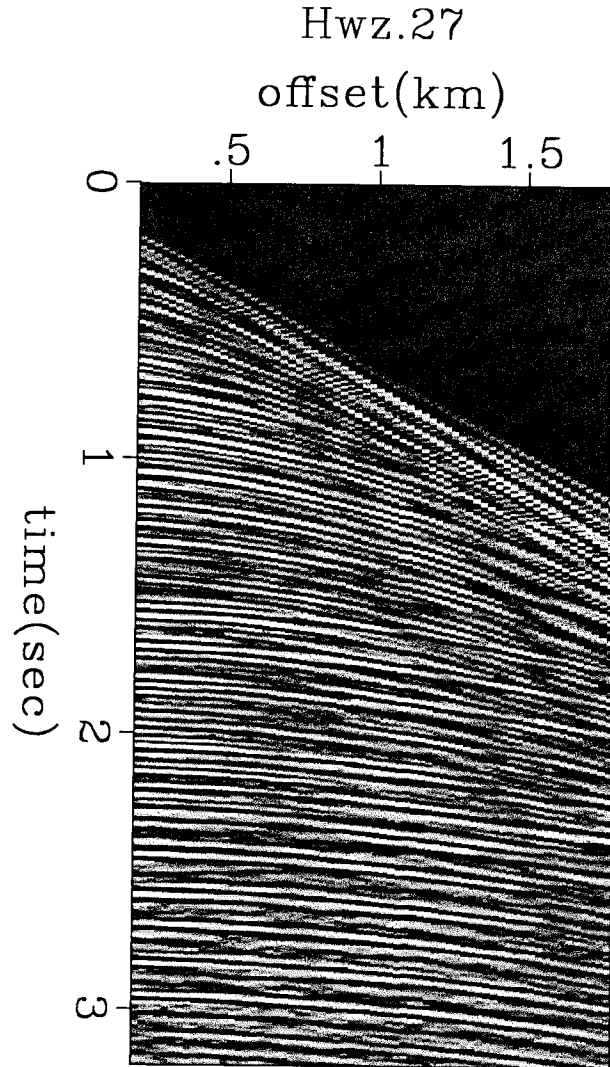


FIG. 3. Marine field data used in this article. From Western Geophysical sample profiles, #27.

$$t = t_0 \left( 1 - p^2 v^2 \right)^{-1/2}. \quad (4)$$

### Snell trace extraction by dip filtering

Kostov and Biondi (1987) solved equations (1) and (2) for the hyperbola passing through each data point. The hyperbola is parameterized by velocity and apex time

$$v = \sqrt{\frac{h}{pt}}, \quad (5)$$

$$t_0^2 = t^2 - pth, \quad (6)$$

or a function of time  $t_1$  and offset  $h_1$

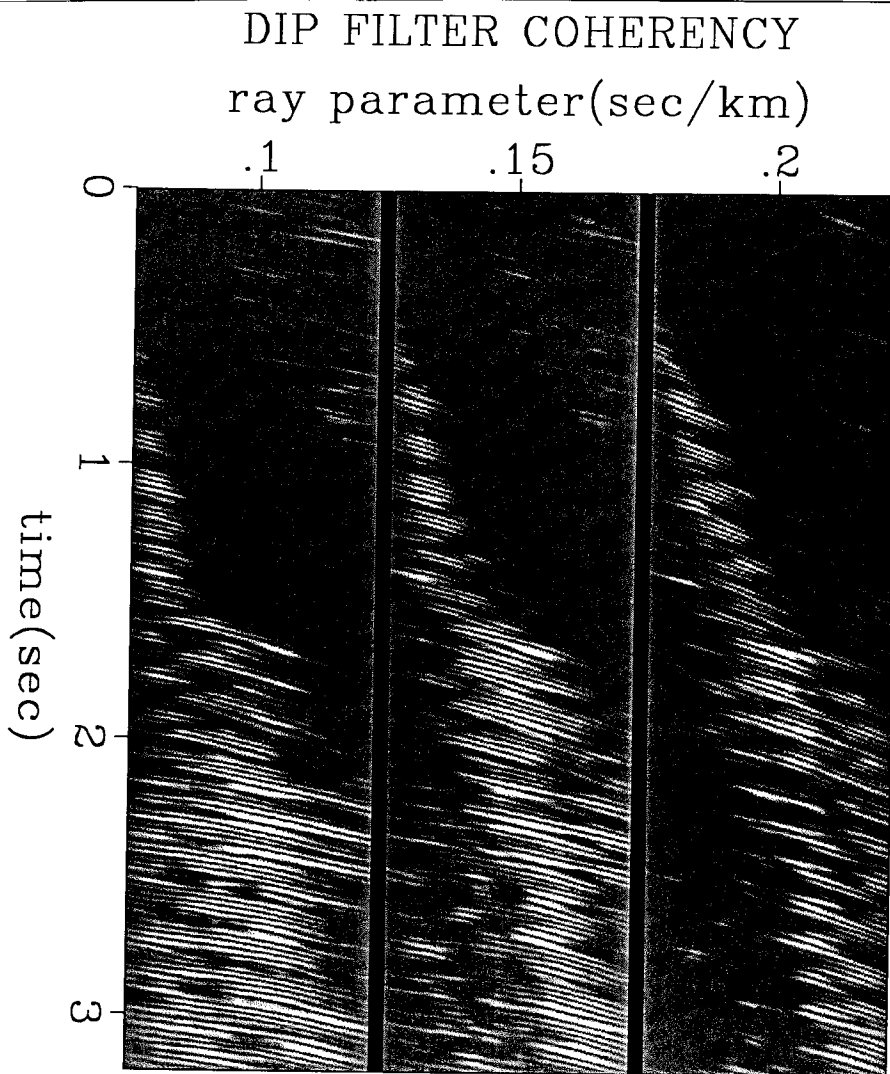


FIG. 4. Semblance measurements of Figure 3 profile for three different time slopes.

$$t_1^2 = t^2 + pt \left( \frac{h_1^2}{h} - h \right). \quad (7)$$

Equation (7) comes from inserting  $t_1$  and  $h_1$  into equations (5) and (6) and then into (1).

Semblance measurements along the equation (7) hyperbolas discriminate equal time slope data, i.e., a Snell trace. This method does not require an *a priori* velocity model as does Ottolini's method. This method resembles Gonzalez's (1982) velocity-dependent linear-moveout migration.

## OFFSET PICKING

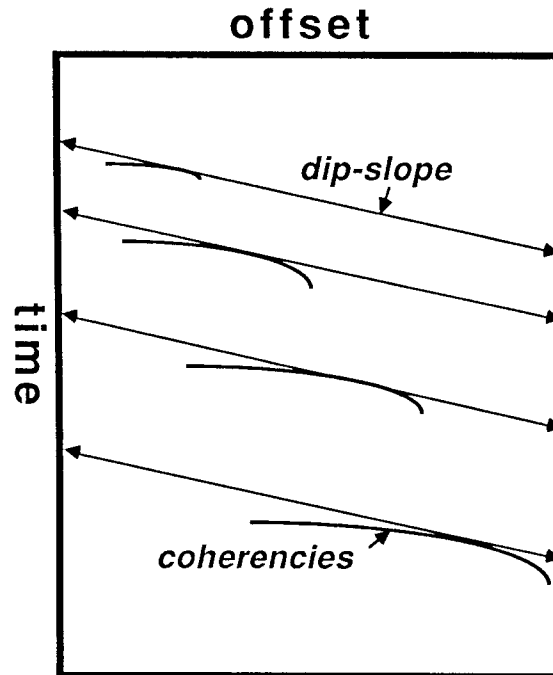


FIG. 5. Offset peak picking schematic. The offset with the largest semblance peak is picked along slope lines for each time point. This offset-time-peak function is then edited to define a Snell trace trajectory.

### Computation and picking

The computation procedure is similar to conventional velocity analysis. The traces of a gather are time stretched accorded to equation (7) and summed over offset (Figure 2). This is repeated at each offset. Figure 4 shows the a marine profile semblance for several time slopes.

The computation cost is four dimensional:  $np$  Snell traces times  $nh$  measurements times  $nh_1$  traces  $nt$  samples long. This is one more dimension than conventional velocity analysis, but the procedure vectorizes well. The number of input traces per output trace,  $nh_1$ , need only be large enough to discriminate signal and less than the entire cable length,  $nh$ . I find  $nh_1=15$  works well.

### Picking

The next step is to pick offset as a function of time. This defines a Snell trace, and via equation (5), simultaneously picks a velocity function. The offset with the largest semblance peak is picked along the slope line for each time point. See the schematic in Figure 5.

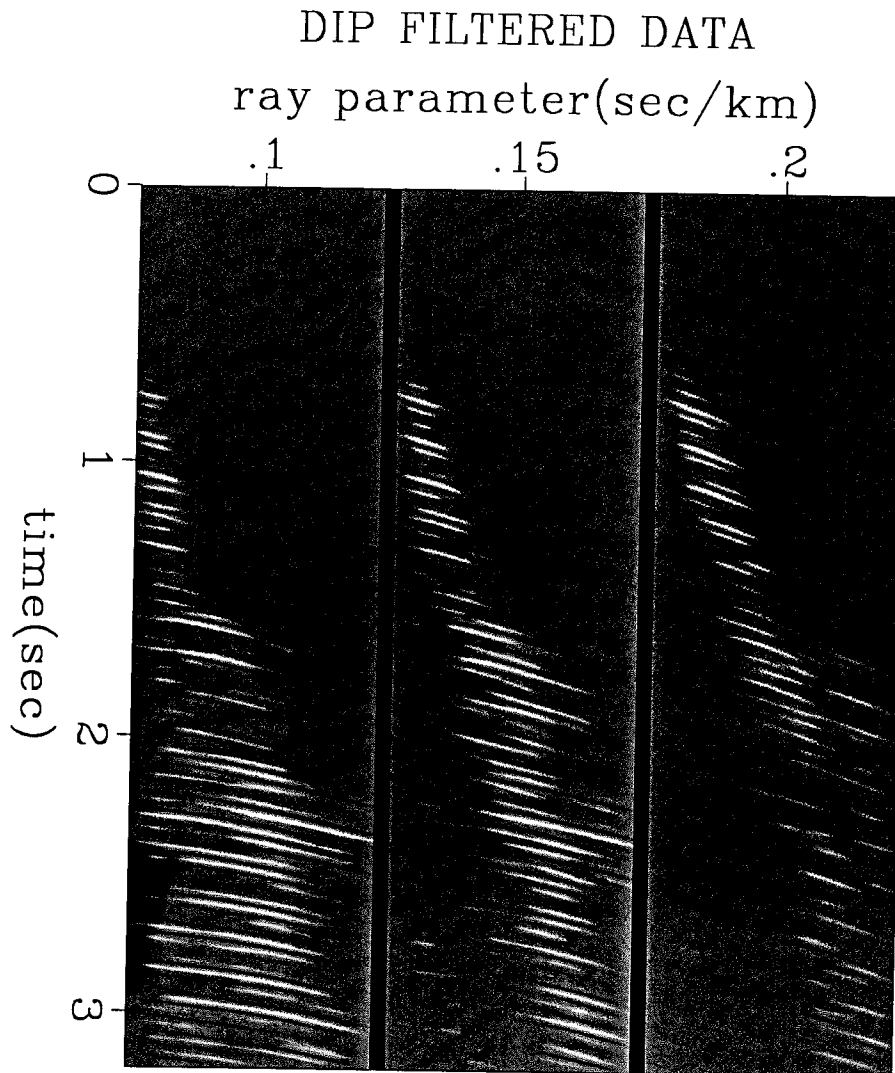


FIG. 6. Semblance weighted data of same profile as Figure 3. This removes some of the non-reflection coherencies for a better peak picking dataset.

The source data for picking can be the semblance (Figure 4), or the dip filtered data (Figure 6), or both. I prefer using the filtered data because it discriminates against some non-reflector dip slopes (difference between Figures 4 and 6).

The raw picked semblance, offsets, and velocities (Figure 7) need both smoothing and error editing. Conventional velocity analysis picking techniques can be applied to Snell trace offset picking: e.g. thresholding, time smoothing, contouring, vrms constraints, interval velocity constraints, and midpoint mixing. There is an additional constraint of a separate event pick and velocity function at each ray parameter. I find time smoothing and velocity constraints to be most useful. I did not try dip mixing and ray-parameter-consistent constraints.

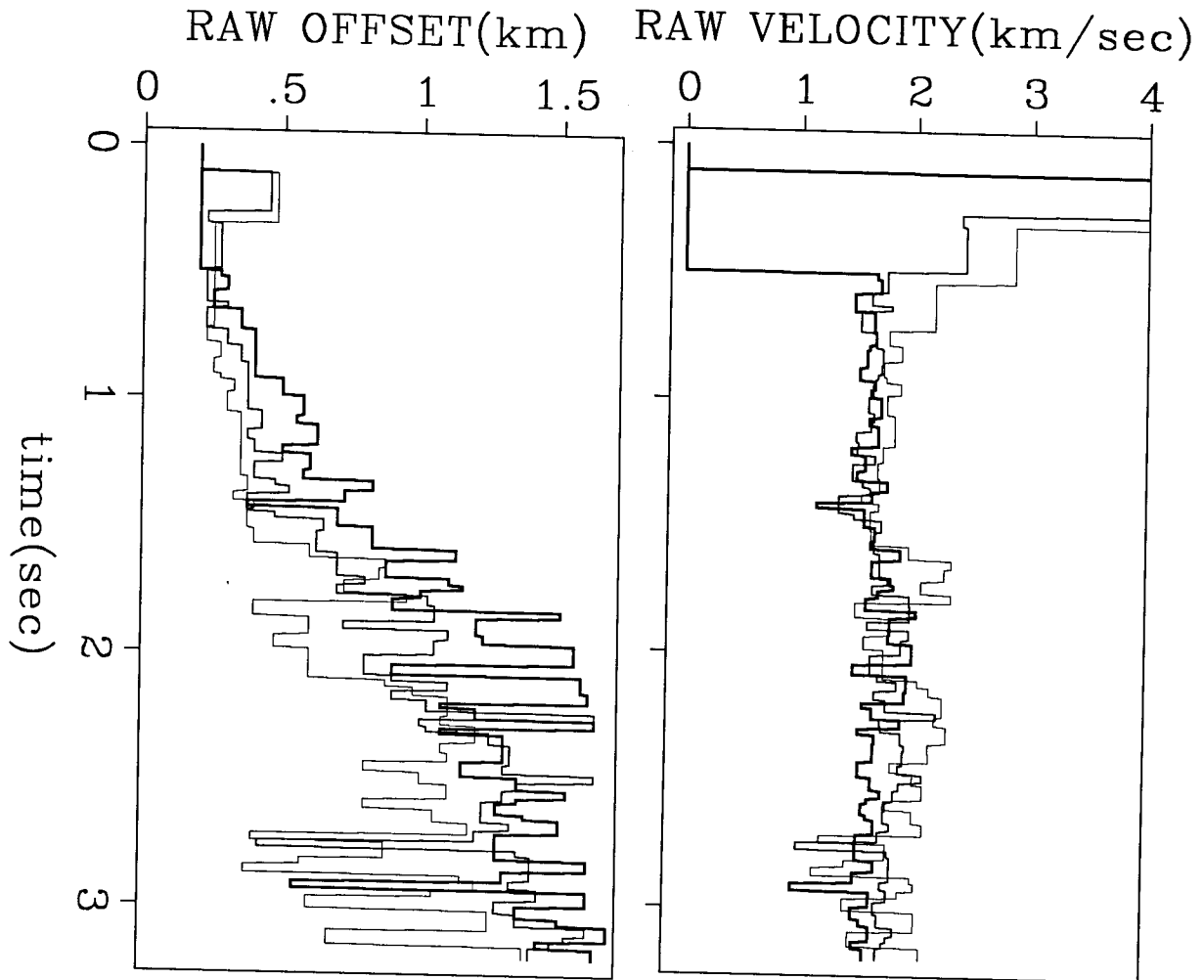


FIG. 7. Raw picked offset and velocity from the Figure 4 data. The thicker the line, the larger the ray parameter.

### Velocity bounds

From equation (5), equal root-mean-square (RMS) velocity contours are diagonal lines from the origin (Figure 8). The minimal and maximal RMS velocities are the shallowest and steepest permissible lines.

Interval velocities are proportional to the slope of the line connecting two picks of a gather (Claerbout, 1977). Inserting equation (5) in Dix's equation gives

$$v = \sqrt{\frac{\Delta h}{p \Delta t}} \quad (8)$$

Constraints on the interval velocity limit the slope between picks (Figure 9).

**RMS VELOCITY BOUNDS**

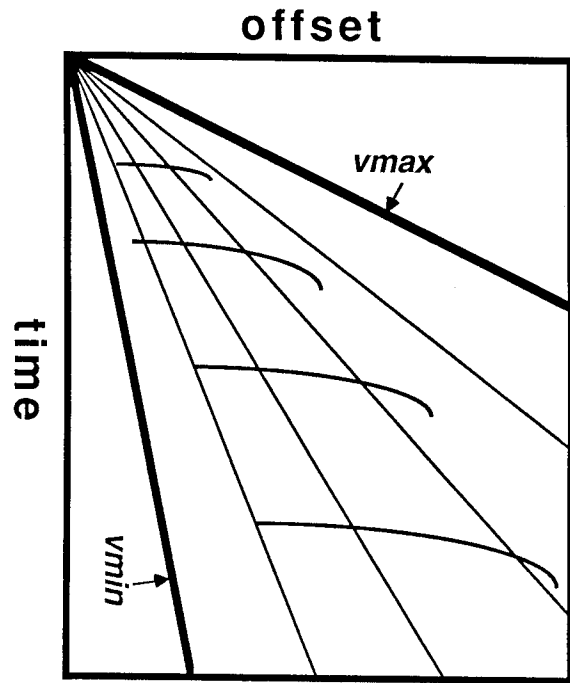


FIG. 8. RMS Velocity bounds for constraining picking of a dip filtered gather. Iso-velocity contours are the diagonal lines given by equation (5). Velocity bounds are based on the lowest and highest lithologic velocities expected, after RMS conversion.

**INTERVAL VELOCITY BOUNDS**

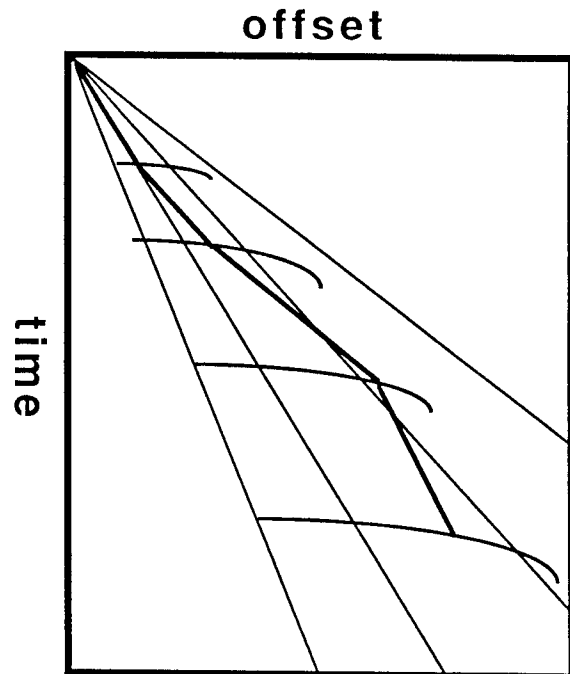


FIG. 9. Interval velocities are related the slope of the line between two picks (equation (8)). Lithologic bounds constrain both the slopes and picks.



## HYPERBOLA TOP BOUNDS

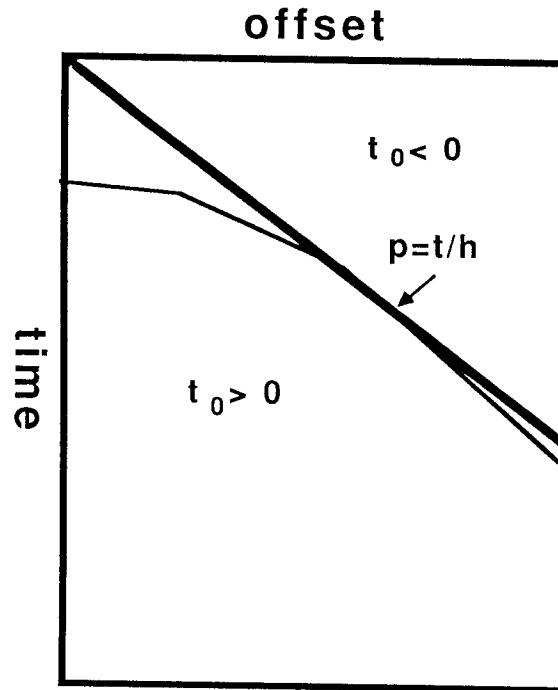


FIG. 10. Semblance hyperbola tops are positive below the iso-velocity contour with the ray-parameter velocity. The negative region generally contains refracted waves rather than reflected waves. It is usually discarded by linear moveout operations.

According to equation (6), semblance hyperbola tops have negative travel time when  $t/h > p$ . The steepest part of a hyperbola, i.e. limb, can't exceed this slope. The minimal hyperbola velocity is bounded by the ray parameter. This bounds is shown on the data in Figure 10. It generally occurs in the refracted wave region rather than the reflected wave region.

### Results

Figure 11 shows the Snell trace picks for the field dataset. Data-driven Snell trace extraction works when there are reflectors to pick. Figure 12 compares the velocity functions defined by the Snell trace picks to a conventional velocity semblance. They are comparable. Angle-dependent variation in the Snell trace velocity picks are caused by the picking variations and non-hyperbolic data moveouts. Adding a ray-parameter-consistent constraints would reduce variations caused by picking. Non-hyperbolic data moveouts can be used to analyze velocity anisotropy.

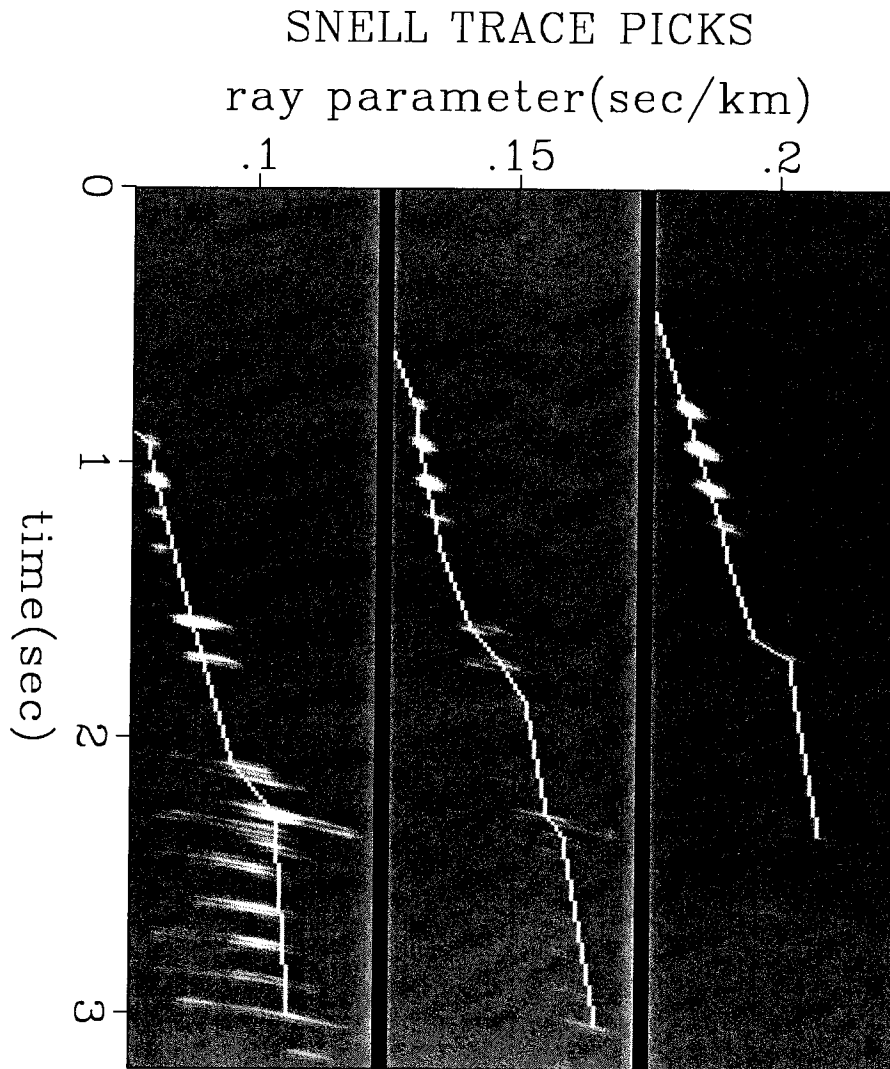


FIG. 11. Snell trace picks derived from Figure 6 data. The smoothed data envelop is displayed beneath the picks. Picks are possible only where there are reflectors. A positive interval velocity constraint avoids multiples in the leftmost panel.

## RELATION TO OTHER SLANT STACK METHODS

### LMO migration, beam stacks, velocity analysis and Snell trace extraction

The linear moveout migration method of Gonzalez (1982), the slant stack enhancement method of Kostov and Biondi (1987), the Snell trace extraction method of this paper, and the beam stacks of Biondi (1987) are mathematically similar. They vary in procedure and results. Gonzalez's method uses finite difference migration instead of hyperbolic summation, uses the full offset aperture rather than partial hyperbolas, and requires a migration velocity function. It has more artifacts than the beam stack methods. After dip filtering, Kostov integrates along linear moveout for better slant stacks, Gonzalez picks peaks for velocity analysis, Ottolini picks peaks for Snell traces,

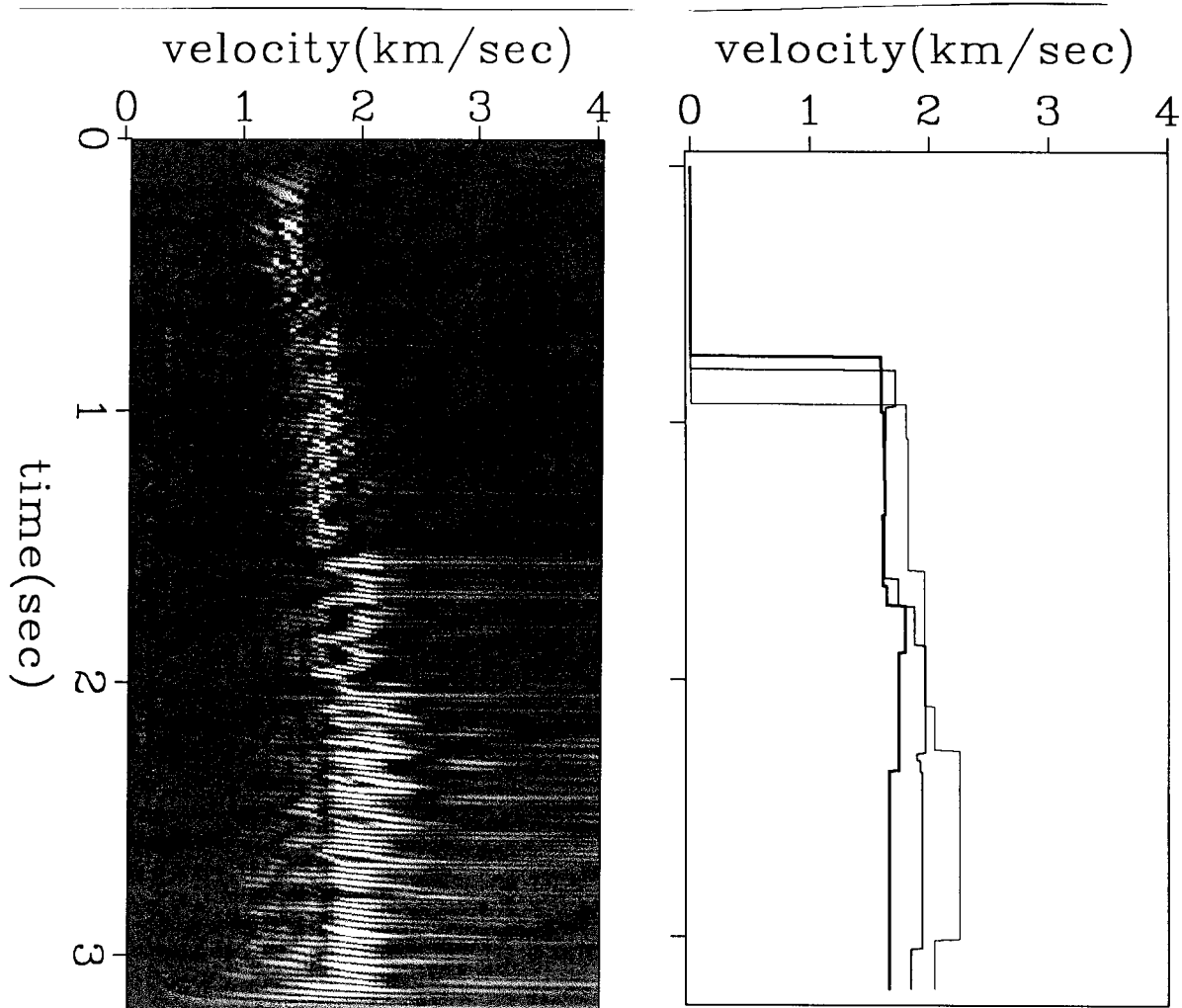


FIG. 12. RMS velocity functions derived two ways: convention hyperbola semblance (left) and via Snell trace extraction (right). They are similar. Both detect velocity increases at .7 seconds and 2.1 seconds. These can be seen in the dip-offset picks (i.e. Snell trace trajectories) of Figure 10.

Snell trace velocity picks are bounded by ray-parameter dependent offset truncations. The near offset boundary truncate low time, while the far offset boundary truncates the high velocity picks.

Variations in the Snell trace velocity functions are caused by picking artifacts and angle-dependent velocity variations.

and Biondo does an optimization-inversion to fit the best velocity model the peaks. In my opinion, Biondo obtains the best velocity analysis, though he loses angle-dependent velocity information.

### Snell traces, CDR, beam stacks and pre-stack migration

The-Snell-trace midpoint-section migration method of Ottolini (1983), controlled-directional-reception of Sword (1987), and beam-stack-migration method of Biondi (1987) are pre-stack migrations of slant stacks. They differ in the number of slant stack dimensions, degree of picking, size of the intermediate data space, and post-slant-stack imaging method. These are summarized in table 1.

Table 1: Three slant stack imaging methods					
NAME	REFERENCE	SLANT STACKS	PICKING	DATA SIZE	IMAGING
Snell trace	Ottolini (1983)	midpoint	offset	medium (3-D)	wave equation migration
CDR	Sword (1987)	midpoint,offset separately	midpoint, offset	small	tomographic optimization inversion
Beam stacks	Biondo (1987)	shot,geophone sequentially	none	large (5-D)	modeling optimization inversion

### CONCLUSIONS

Data-driven Snell trace extraction is a viable alternative to model-driven Snell trace extraction. It is velocity independent and simultaneously picks an angle-dependent velocity function. It works only when there are reflections to pick and adds the cost of filtering.

Data-driven Snell trace extraction is potentially a tool for analyzing angle dependent data effects such as offset-amplitude variations and velocity anisotropy.

### REFERENCES

- Biondi, B., 1987, Interval velocity estimation from beam stacked data: SEP-51  
 Claerbout, J.F., 1977, How to measure interval velocities with a pencil and straight-edge: SEP-11, p.41-44  
 Gonzalez-Serrano, A., 1982, Wave equation velocity analysis: PhD thesis, SEP-31  
 Kostov, C., and Biondi, B., 1987, Improved resolution of slant stacks using beam stacks: SEP-51  
 Ottolini, R., 1983, Migration of reflection seismic data in midpoint-angle coordinates: PhD thesis, SEP-33  
 Ottolini, R., 1986, Slant stacks from velocity stacks: SEP-48, p.295-300  
 Sword, C.H., 1987, Tomographic determination of interval velocities from seismic data via the CDR method: PhD thesis, Stanford University (also portion in SEP-51)